Nano Energy 60 (2019) 404–412

Contents lists available at ScienceDirect

Nano Energy

journal homepage: www.elsevier.com/locate/nanoen

Full paper

Macroscopic self-assembly network of encapsulated high-performance triboelectric nanogenerators for water wave energy harvesting

Xiaodan Yang[a,b,1], Liang Xu[a,b,1], Pei Lin[a,b], Wei Zhong[a,b], Yu Bai[a,b], Jianjun Luo[a,b], Jian Chen[a,b], Zhong Lin Wang[a,b,c,*]

[a] CAS Center for Excellence in Nanoscience, Beijing Key Laboratory of Micro-nano Energy and Sensor, Beijing Institute of Nanoenergy and Nanosystems, Chinese Academy of Sciences, Beijing, 100083, China
[b] School of Nanoscience and Technology, University of Chinese Academy of Sciences, Beijing, 100049, China
[c] School of Material Science and Engineering, Georgia Institute of Technology, Atlanta, GA, 30332, USA

ARTICLE INFO

Keywords:
Self-assembly
Triboelectric nanogenerator network
Water wave energy harvesting
Self-adaptive magnetic joint
Three-dimensional electrode

ABSTRACT

Water wave energy is one of the tremendous clean energy reserves on earth. The utilization of wave power has long been focused but at limited scope due to challenges such as cost and durability in severe ocean environment. Here, a macroscopic self-assembly network of encapsulated triboelectric nanogenerators (TENGs) is proposed for the first time for water wave energy harvesting. By a rationally designed self-adaptive magnetic joints, the network demonstrated capabilities of self-assembly, self-healing and facile reconfiguration, greatly improving the autonomy and robustness of the system. A three-dimensional electrode structure boosts the output of the TENG unit, with an *average power density* of 8.69 W m^{-3} under ideal agitations and 2.05 W m^{-3} in water waves, which is more than 18 times of the power of the reported ball-shell structured device despite lower agitation frequency here. The self-assembly TENG network as a robust and high-performance structure should provide a reliable route towards large-scale utilization of the water wave energy, enabling self-powered systems in ocean.

1. Introduction

Water wave energy, abundant in ocean, is considered as a promising source for the ever-growing needs of renewable and clean energy of human society [1–3]. According to an estimation, the wave power around the coastline can reach more than 2 TW (1 TW = 10^{12} W) globally [4,5]. Although large efforts have been made for exploiting such huge amount of energy for decades, rare commercial advancement has been achieved [1,3,6]. The challenge largely lies in the cost and durability of the equipment. Current experimental machines based on electromagnetic generators usually need sophisticated mechanical structures to catch and convert waves to highly regular motions for driving the generator, thus they are often bulky, costly and vulnerable in severe ocean environment [1–3,7]. The triboelectric nanogenerator (TENG) provides a different route towards the goal [8–10]. Theoretically derived from the Maxwell's displacement current, the TENG exhibits merits of easy fabrication, low cost and versatile material and structure choices [11]. It is proven to be highly effective to harvest low-grade, low-frequency and disordered mechanical energies, such as walking, wind, vibration and water waves [9,11–16]. The concept of using the TENG and its network to harvest wave energy was first proposed in 2014 [9,10]. Since then a number of prototypes have shown its feasibility in principle [5,17], and networking has also been proven to be a significant strategy for coupling TENG units in water to achieve a high efficiency [13]. Despite of these progresses, practical application of large-scale TENG networks in ocean could involve hundreds of thousands of units, which brings complexity in the construction and maintenance. Meanwhile, the network would also be threatened by severe ocean environment, such as storms, which can easily break large structures in ocean. The connection between units through strings or similar structures can also suffer from fatigue failure by alternating stress in long-term running. Thus an advanced design that can adapt to these challenges is required.

Self-assembly is a process where disordered components in a system aggregate together to form certain patterns or structures based on local interactions among components [18–23]. It is a natural phenomenon

* Corresponding author. CAS Center for Excellence in Nanoscience, Beijing Key Laboratory of Micro-nano Energy and Sensor, Beijing Institute of Nanoenergy and Nanosystems, Chinese Academy of Sciences, Beijing, 100083, China.
E-mail address: zhong.wang@mse.gatech.edu (Z.L. Wang).
[1] These authors contributed equally to this work.

https://doi.org/10.1016/j.nanoen.2019.03.054
Received 25 January 2019; Received in revised form 1 March 2019; Accepted 14 March 2019
Available online 19 March 2019
2211-2855/

widely observed in different scales from molecules to large-scale weather systems. As a practical synthetic strategy in molecular or nano-scale, it attracts increasing interests from multiple disciplines as chemistry, biology, and material science, to fabricate ordered aggregates beyond the covalent bond [18–20]. For larger sizes concerning meso- or macro-scale, attempts have also been conducted to construct highly autonomous systems mimicking the analogs in small scales, such as interconnected electrical networks, robotics systems and so on [21–24]. In principle, the self-assembly provides a universal strategy for construction of ordered complex structures containing massive simple elements without human intervention, and the system is usually featured by self-healing due to the reversibility of the binding. Such characteristics are highly desired for large-scale TENG networks in ocean, and there is also a possibility considering that the water environment allows the mobility of the units and the wave can offer an agitation source. Adopting self-assembly as the netting strategy could enable a TENG network that is more adaptive to the ocean environment, though realizing self-assembly in such a scale when maintaining the performance of energy harvesting is challenging.

Here, we present a self-assembly TENG network based on encapsulated high-performance units for water wave energy harvesting. The self-assembly is realized through a self-adaptive magnetic joint (SAM-joint) which operates on a self-adaptive mechanism of the pole and an anisotropic restriction on the degree of freedom. The pattern of the self-assembly structure can be tuned by the amount of SAM-joints on each unit that introduces geometrical information. The network also exhibits capabilities of self-healing up ruptures and facile reconfiguration. These features should greatly enhance the autonomy and mechanical robustness of the network, facilitating large-scale fabrication and maintenance. The basic component TENG unit of the network adopts an encapsulated three-dimensional (3D) electrode structure with intercalated pellets, which is demonstrated to boost the output with an average power density of 8.69 $W m^{-3}$ under ideal agitations and 2.05 $W m^{-3}$ in water waves. The presented network as a self-assembly energy harvesting system provides a useful strategy towards utilization of the wave power. The method should also be widely applicable for the construction of other large-scale marine structures.

2. Results and discussion

2.1. Self-assembly TENG network

The concept of self-assembly of TENG units is schematically illustrated in Fig. 1a. Agitated by water waves, scattered spherical TENG units can spontaneously assemble together to form a network with specific patterns through stochastic approaching and the interaction of assembly joints. Such self-assembly behavior imparts the multiple-TENG system highly autonomous abilities which could greatly lighten the cost to fabricate and manage the network [25]. Based on the reversibility of the connection, the network is also capable of self-healing up after a rupture occurs in extreme conditions, such as in storms, where temporary detachment of adhered joints would protect the TENG units from permanent damage. Thus the mechanical robustness of the system could be dramatically improved. The morphology of the network may also be readily reconfigured upon reconnection of assembly joints to achieve certain network arrangements.

2.2. Structure and working principle of the TENG unit

To realize the self-assembly TENG network, an encapsulated high-performance TENG unit with 3D electrodes and SAM-joints is designed. The structure of the device is schematically presented in Fig. 1b. A 3D electrode ball constituted by a group of electrode plates are sealed by a spherical shell, where the copper layers on the electrode plates are connected together which consequently form a pair of 3D electrodes on the substrates. Fluorinated ethylene propylene (FEP) pellets are intercalated into the internal channels of the 3D electrode ball as a tribo-material. SAM-joints featured by a rotatable spherical magnet and a limit block are mounted around the periphery of the shell. Fig. 1c and d shows photographs of fabricated 3D electrode balls and the TENG unit, respectively. Detailed fabrication process of the self-assembly TENG unit is described in the Experimental Section. The self-assembled network by the fabricated units is shown in Fig. 1e.

The working mechanism of the TENG is based on the conjugation of tribo-electrification and electrostatic induction [11]. As shown in Fig. 1f, when the TENG is agitated by external mechanical excitations, such as water waves, the FEP pellets will roll and shuttle between the two 3D electrodes along internal channels. The surface of the FEP pellets will be negatively electrified due to higher affinity to negative charges compared with copper electrodes [26,27], which are positively electrified. The back-and-forth motion of the electrified FEP pellets will induce free electrons to move accordingly between the two 3D electrodes through an external circuit, producing an alternating current. The mechanical energy to drive the pellets are thus converted to electrical energy.

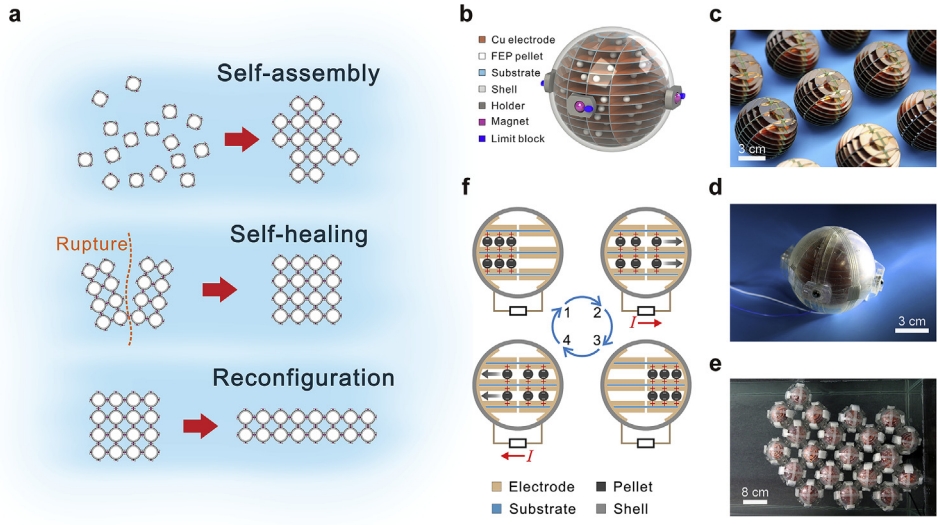

Fig. 1. Structure design and working principle. (a) Schematic illustration of self-assembly, self-healing and reconfiguration of the network. (b) Schematic structure of the TENG unit. (c–e) Photographs of internal 3D electrode balls (c), the TENG unit (d) and the self-assembled TENG network in water (e). (f) Working principle of the TENG.

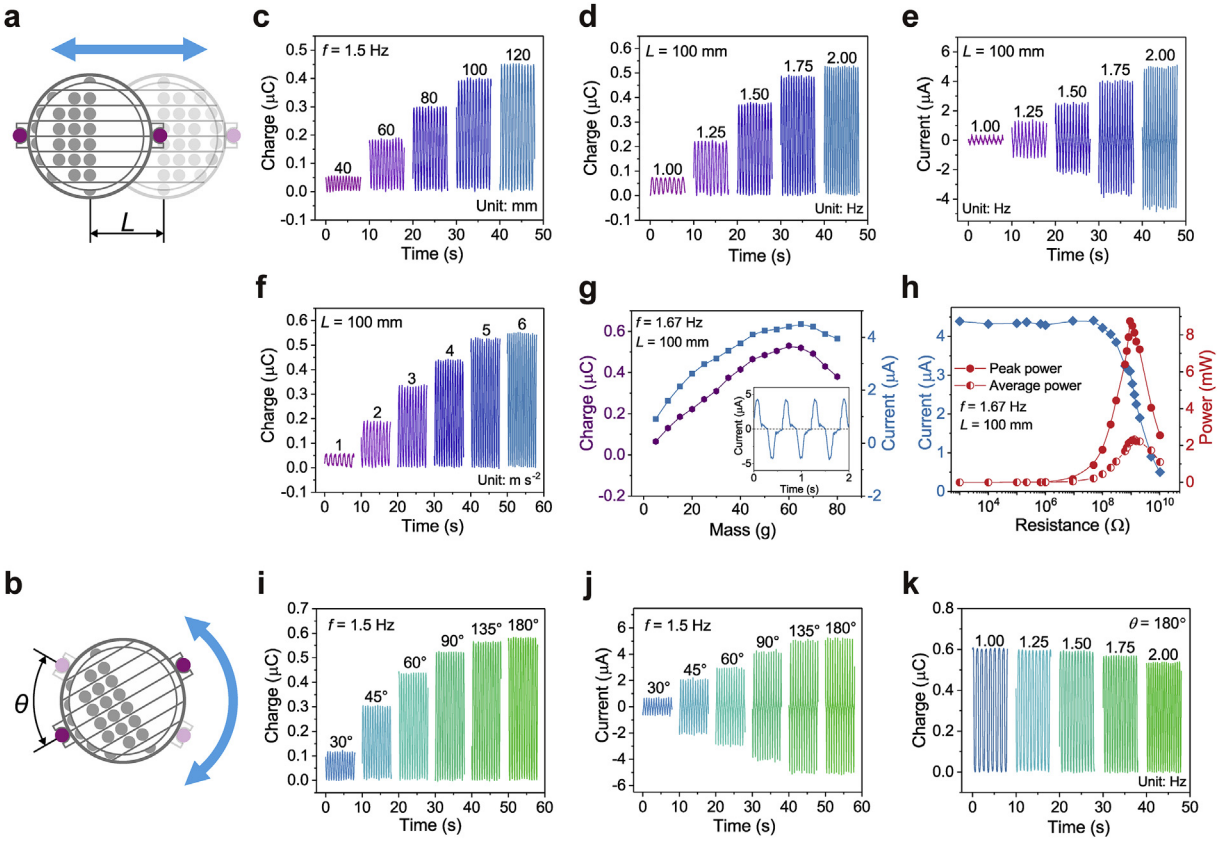

Fig. 2. Electrical output performance of the TENG under translational and pitching agitations in air. (a, b) Schematic diagrams of two modes of agitations. (c) Dependence of short-circuit transferred charges on the displacement extent of translational harmonic agitations. (d, e) Dependence of transferred charges (d) and short-circuit current (e) on the frequency of translational harmonic agitations. (f) Dependence of transferred charges on the acceleration of translational impact agitations. (g) Influence of the amount of FEP pellets on transferred charges and peak short-circuit current of the TENG under translational impact agitations. Inset: profile of the short-circuit current. (h) output power and peak current versus load resistance under translational impact agitations. (i, j) Dependence of transferred charges (i) and short-circuit current (j) on the angular displacement extent of pitching harmonic agitations. (k) Dependence of transferred charges on the frequency of pitching harmonic agitations.

2.3. Characterization of a single TENG unit

The FEP pellets inside the 3D electrodes can be agitated by various external excitations based on inertial force or gravity. Two typical modes, namely the translational mode and the pitching mode, are adopted to characterize the output performance of the TENG unit, as shown in Fig. 2a and b. For the translational mode, harmonic agitations with different displacement extents L and frequencies f were imposed on the unit by a linear motor at first. The short-circuit transferred charges Q_{SC} and short-circuit current I_{SC} were characterized as shown in Fig. 2c–e. With increasing displacement extent or frequency, the transferred charges and current also rise rapidly. A peak output of 0.52 μC and 5 μA is achieved under the condition $L = 100$ mm and $f = 2$ Hz, which is far larger (over 7 times for the charge output) than previously reported ball-shell-structured device [13,17], and the output is acquired without any corona charging process [28]. The boost of output should originate from much larger contact interface by adopting 3D electrodes. Besides the harmonic agitation, impact is another representative agitation form. We tested the transferred charges of the TENG under different impact accelerations a (Fig. 2f). The output increases with larger acceleration and reaches 0.55 μC at 6 m s^{-2}. We also studied the dependence of the electrical output on the mass of the FEP pellets in a single TENG unit. As shown in Fig. 2g, the peak short-circuit current and transferred charges both demonstrate a non-monotonic variation as the mass increases from 5 g to 80 g. The outputs reach maximum at around 65 g, where the FEP pellets can fill nearly exactly half of the volume of each internal channel of the 3D electrode ball. With more FEP pellets, the other half of the internal channels starts to be filled up, and the electrostatic induction effect on the two 3D electrodes will cancel out partially. The inset of Fig. 2g shows that the current output of the device has much wider peaks than contact-separation-mode devices which is in favor of larger ratio of average to peak power [29]. The dependence of peak current I_{peak}, peak power P_{peak} and average power P_{ave} on different resistive loads R are shown in Fig. 2h. The average power was calculated according to

$$P_{ave} = \frac{\int_0^T I^2 R dt}{T} \quad (1)$$

where T is the period of the output and I is the output current. A maximum peak power of 8.75 mW and maximum average power of 2.33 mW are attained with a matched impedance of around 1 GΩ under translational impact agitations of 1.67 Hz. Considering the TENG ball has a volume of 2.68 × 10^{-4} m^3, a peak power density of 32.6 W m^{-3} and an average power density of 8.69 W m^{-3} can be delivered. Due to that the peak power is only a transient output of the device, the average power can reflect the energy harvesting performance more exactly, and the value achieved here is much higher than previously reported results of similar devices, more than 18 times of the average power of the recently reported ball-shell structured device despite the latter was tested with an higher operation frequency of 3 Hz [13]. The output voltage of the TENG while connecting resistive loads is also calculated based on the measured current, as shown in Fig. S1. It demonstrates that the device has high open-circuit voltage which should be important considering the figure-of-merit of the device [30].

For the pitching mode, the influence of angular displacement extent θ and frequency f under harmonic agitations has been studied. With increasing angular displacement extent, the peak values of transferred charges and short-circuit current both rise rapidly and saturate at around 180° with 0.58 μC and 5.2 μA, respectively (Fig. 2i and j). The transferred charges decrease a bit with larger frequencies (Fig. 2k), which could be attributed to the insufficient contact of the FEP pellets with the electrode surface in a high-frequency pitching motion.

2.4. Operation principle of the SAM-joints

Magnetism is a commonly adopted interaction force in a macroscopic self-assembly system, and the reported assembly unit usually has a simple form with one magnetic dipole [25]. Such form is not applicable for the TENG unit due to the large size and complex structure. A design with multiple small magnets distributed around model balls (in substitution for the TENG ball for simplicity in self-assembly experiments) was tested at first, which demonstrated a poor performance, as shown in Fig. S2 in the Supplementary Information. Large amount of assembly errors appeared in the self-assembly network where magnets with the same outside pole attached together from the edge (Fig. S2c, Supplementary Information). This resulted in a severely distorted pattern of the network. Moreover, the attachment of the magnets is almost a rigid connection without any degree of freedom which is adverse to wave energy harvesting [13]. To solve these problems, we designed the SAM-joints shown in Fig. 1b where the spherical magnet can rotate freely in the holder. The operation principle of the SAM-joints is based on a self-adaptive mechanism of the pole and an anisotropic restriction on the degree of freedom. As shown in Fig. 3a, for arbitrary initial orientations of the magnets, once the two joints are close enough, the spherical magnets will quickly rotate and self-adjust to the state with opposite poles outside and get attached due to magnetic interaction. Thus the magnets can always assemble together at the right position. Such self-adaptive mechanism of the pole also ensures a larger assembly probability because two arbitrary joints can complete the attachment without distinguishing the poles. A detailed attachment process is demonstrated in Supplementary Video S1. To investigate the connection strength, the magnetic attracting force between two joints was both measured and numerically calculated by COMSOL, as shown in Fig. 3b and c. A higher magnetic force can be obtained with a smaller distance D and a larger diameter of the magnet H. The attracting force is above 6 N for the adopted 8 mm magnet in attached state experimentally.

Supplementary video related to this article can be found at https://doi.org/10.1016/j.nanoen.2019.03.054.

In order to introduce flexibility for energy harvesting performance while maintaining the assembly structure of the network, a limit block is designed as shown in Fig. 3d and e, which has a larger size in horizontal dimension than in vertical dimension, for an anisotropic restriction on the degree of freedom. Two limit blocks in an assembled junction can almost completely restrict the rotation in horizontal direction (Fig. 3d). The center of the two units and the junction will keep in line, thus the designed pattern of the network can be guaranteed. For the vertical direction, due to the smaller size of the limit block in this direction, adjacent units can have relative rotation freely in a range (Fig. 3e), which is also consistent with the aforementioned pitching motion. Therefore, the network can interact with water waves effectively and harvest wave energy.

2.5. Self-assembly, self-healing and reconfiguration of the network

With the SAM-joints, the units are able to self-assemble into networks with certain patterns of structure. By introducing structure information with different amounts and distributions of the SAM-joints on each unit, the pattern can be designed. We investigated the influence of the amount of joints on the pattern. Typical units and theoretical predicted small self-assembly modules and networks are presented in Fig. 4a–c. The prediction is based on the geometrical restriction that the center of neighboring units and their attached junction should keep in line. The resulted modules and networks are straightforward: Two-joint units can form a dimer which may extend to a number of linear chains (Fig. 4a); three-joint units can form a small module of “hollow” hexagon and a network constituted by such pattern (Fig. 4b); four-joint units can provide a square cluster which can expand to a network (Fig. 4c).

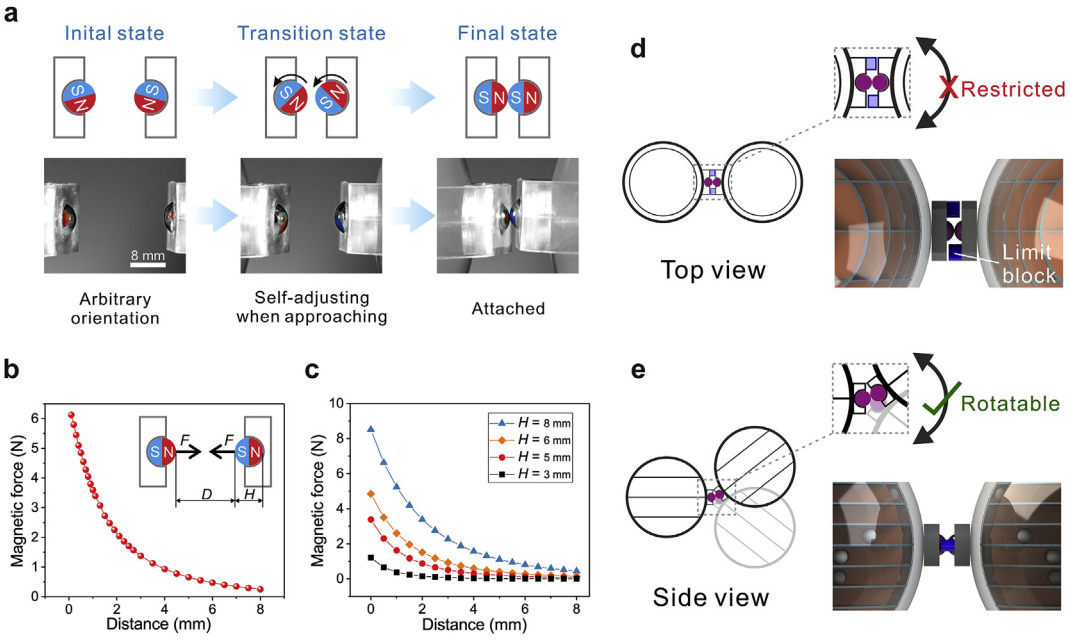

Fig. 3. Working principle of the SAM-joint. (a) Schematic illustrations and photographs of the self-adjusting and attaching process of two SAM-joints (without the limit block). (b) Measured attracting force of two joints under different separation distances. Inset: schematic diagram of the joints and the attracting force. (c) Numerically calculated attracting force of two joints by COMSOL. (d, e) Schematics of the attached joints which only allow relative motion of the TENG units in the vertical direction.

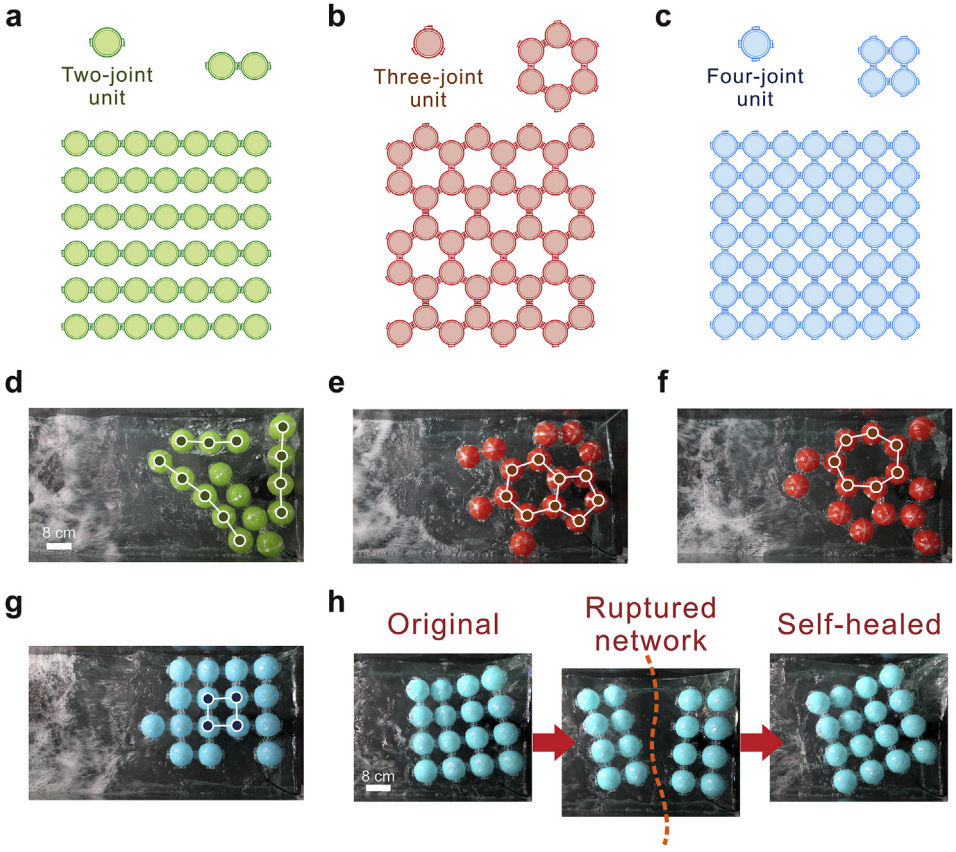

Fig. 4. Self-assembly and self-healing behavior of the network. (a–c) Schematic illustrations of theoretical structures of self-assembled small modules and TENG networks with two-joint units (a), three-joint units (b) and four-joint units (c), respectively. (d–g) Photographs of typical self-assembled networks agitated by water waves for two-joint units (d), three-joint units (e, f) and four-joint units (g), respectively. (h) Photographs of the self-healing process of the network in water.

Based on the theoretical analysis, we further investigated the self-assembly behaviour of different types of units in a real water circumstance with water waves. For the convenience of fabrication, model balls which have the same size with the TENG units were used here. Three types of units were experimented. While released into the wave tank successively and agitated by water waves, the units quickly self-assembled into networks with patterns based on the amount of joints on each unit. As shown in Fig. 4d–g, the resulted typical networks and small modules extracted from the networks conform well to theoretical predictions with some small deviations: The chain by two-joint units has a minor curvature which can lead to a ring if the chain is long enough; pentagons and heptagons appear in the network of three-joint units besides hexagons. Such deviations may be attributed to tiny clearances around the limit blocks which can allow two adjacent units to rotate a bit horizontally. In the self-assembly experiments, some defects can appear in the network, such as vacancies or coexistence of multiple assembly structures, which could be further suppressed with longer time and higher agitations. More details on the self-assembly process are provided in Fig. S3 and Supplementary Videos S2–S4, and Fig. S4 in the Supplementary Information shows some perfect assembly structures. We also tested other methods to release the units, such as releasing all the units in the wave tank simultaneously or releasing pre-assembled small modules, which can also successfully self-assemble together (Supplementary Videos S5 and S6). Network patterns for units with other joint configurations can be further predicted similarly, as we demonstrate a six-joint unit that should form small modules of triangle and “solid” hexagon and assemble into a densely-arranged network (Fig. S5, Supplementary Information). Moreover, the self-assembly behavior is validated for real TENG units as shown in Supplementary Video S7, which proves that the self-assembly can be practically applied. Although the amount of units used here in the experiments is relatively small, it can be easily scaled up to large networks.

Supplementary video related to this article can be found at https://doi.org/10.1016/j.nanoen.2019.03.054.

The SAM-joints and the self-assembly mechanism enable dynamic and active connections of the network. Due to that the attachment is reversible, self-healing and facile reconfiguration can be realized, which should greatly enhance the mechanical robustness of the network in extreme ocean environments and facilitate the fabrication and maintenance of the network. Fig. 4h, Fig. S6 and Supplementary Videos S8 and S9 demonstrate typical self-healing processes of the network in water. When the network suffers from excessive external energy, the connection between adhered SAM-joints will temporarily break up and absorb some of the energy, which can protect other parts of the network from permanent damage, and the ruptured connections will heal up afterwards through the self-assembly mechanism. The self-healing capability is meaningful for the network to adapt to the oceanic extreme weather which can always threat the survival of marine devices, lowering the cost of maintenance. We also demonstrate the reconfiguration of the network in Fig. S7 in the Supplementary Information, where chains of two-joint units can be assembled into different isomers readily by reconnecting the SAM-joints, enabling convenient active control and reorganization of the network.

Supplementary video related to this article can be found at https://doi.org/10.1016/j.nanoen.2019.03.054.

2.6. Performance of the self-assembly TENG network in water

The wave energy harvesting performance of the self-assembly TENG network was investigated in wave tank experiments. As shown in Fig. 5a, the working principle of the network in water is based on the pitching motion agitated by water waves, which is allowed by the SAM-joints. The four-joint unit is adopted for the experiment for it can form regular high-coverage pattern with a relative simple structure. A network of 4 × 9 array was assembled with 2 × 9 TENG units and 2 × 9 model balls. The 18 TENG units were electrically connected in the

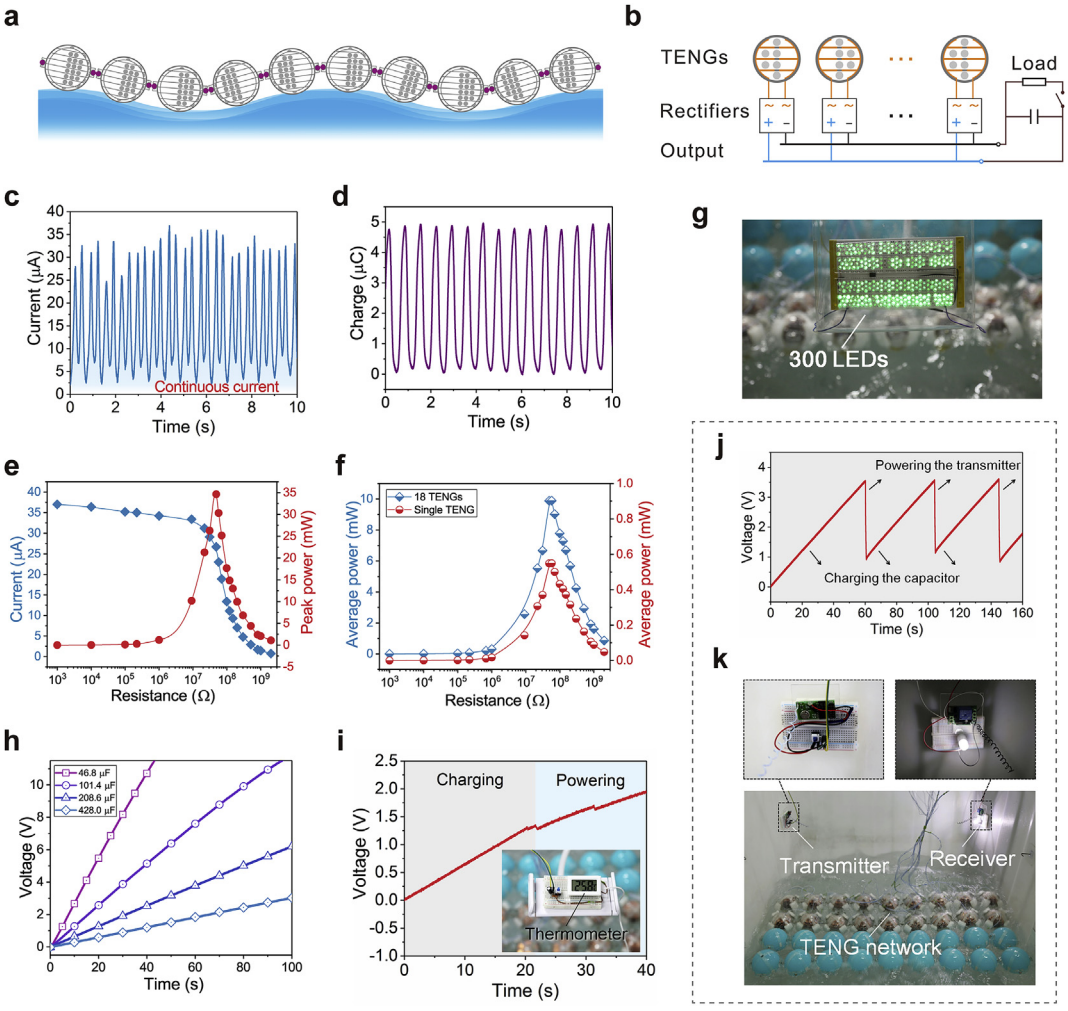

Fig. 5. Energy harvesting performance and application demonstrations of the self-assembly TENG network in water. (a) Schematic illustration of the TENG network agitated by water waves. (b) Schematic diagram of the electrical output circuit for the network. (c, d) Short-circuit current (rectified) (c) and transferred charges (d) of the self-assembly TENG network in water. (e, f) Dependence of peak current, peak power (e) and average power (f) of the self-assembly TENG network on load resistance under water wave agitations with a period of 0.69s. (g) Photograph of 300 LEDs lighted by the network. (h) Charging performance of the self-assembly TENG network to different capacitors. (i, j) Charging-discharging curve of the capacitor for the network to power a thermometer (i) and a wireless transmitter (j). Inset: the thermometer powered by the network. (k) Photographs of the self-assembly network to power the wireless transmitter.

manner shown in Fig. 5b, where rectifiers are used to suppress the negative effect of phase mismatch in the alternating output of different TENG units, then the output are connected together in parallel. The generated electricity can be further used to charge a capacitor and supply power for a load. Due to the limit of dimensions, the wave tank can generate relative strong water waves around a period of 0.69s (1.45 Hz in frequency), which was adopted for experiments here, and the rectified short-circuit current of the network also reaches the maximum near this period (Fig. S8, Supplementary Information) by stronger agitations. The wide current peak can reach above 35 μA with a base continuous current about 2.5 μA (Fig. 5c). The total transferred charges without rectification is 4.9 μC (Fig. 5d), which is equal to 0.27 μC for each TENG unit. The smaller charge output as compared with the result in air could be attributed to that the agitation in water is not so ideal as that driven by a motor and the TENG is not fully excited, which can be improved by imposing stronger agitations in a better wave environment. We also verified the coupling effect of the network as discussed previously [13], by testing non-networked free TENG units in the wave tank (Fig. S9, Supplementary Information). The output is unstable and very low in most of the time for the non-networked unit, which indicates the crucial role of networking for the device. Fig. 5e and f shows the dependence of peak current and power output on load resistance. A peak power of 34.6 mW and an average power of 9.89 mW for the network can be achieved with a matched impedance around 50 MΩ. It is noted that the matched impedance for the network is approximately 1/18 of that of a single TENG, thus by parallel connecting TENG units, the matched impedance can be lowered and tuned, which can better meet the requirement of application loads that always have a low impedance. The average power per unit is about 0.55 mW, corresponding to an average power density of 2.05 W m^{-3} (Each TENG ball has a volume of 2.68×10^{-4} m^3). The achieved power outputs demonstrate excellent performance of the TENG unit and the network as compared with existing similar devices for which the average power in water is rarely reported [5,13,17].

With the generated electricity, the network can be applied for various electronic devices and applications to fabricate self-powered systems agitated by water waves [11]. As an intuitive demonstration, 300 LEDs were easily lighted up by the network as shown in Fig. 5g and Supplementary Video S10. The harvested energy can also be stored in capacitors (Fig. 5h) or batteries to supply power intermittently to devices with relative high power consumption. Two such systems are demonstrated here, as shown in Fig. 5i–k. First, a self-powered thermometer is presented in Fig. 5i and Supplementary Video S11. After charging a capacitor (216.7 μF) from 0 V to 1.33 V within 21 s and

closing the switch, the network can power the thermometer continuously to measure the temperature of the water. The rising voltage of the capacitor in powering portion implies that the harvested energy excesses the consumption. The network is also demonstrated to power a wireless transmitter with a capacitor of 236.6 μF charged to about 3.5 V. The powered transmitter would send a signal which can be received by the receiver to turn on a LED bulb, as shown in Fig. 5j and k and Supplementary Video S12. Moreover, by applying a power management module, the charging efficiency has a great potential to be further improved [31].

Supplementary video related to this article can be found at https://doi.org/10.1016/j.nanoen.2019.03.054.

As shown above, the self-assembly TENG network demonstrates extraordinary performance in water environment, which is expected to effectively harvest large-scale water wave energy in ocean. The harvested power can be applied locally for self-powered systems, or transferred to small islands or the land through submarine cables [10]. The self-assembly, self-healing and reconfiguration capabilities guarantee high autonomy of the network which can facilitate construction and maintenance, largely reducing the cost. In the construction, thousands of units can be transported without any network structure, and they can self-assemble into a network by simply pouring into the water. The rupture of the connection in the network in extreme weather can self-heal up again, preventing permanent damage. Meanwhile, the morphology of the network may be easily controlled through reconfiguration. However, before practical application, there are still some issues to be further investigated: Floating barrier structures may be needed to restrict around the boundary of the network to stop the unit from drifting away, and electrical connections should be further integrated into the SAM-joints to gather the electricity of each unit together, if it is not used locally such as hydrogen generation or sea water desalination. Further investigations are also required to provide a better control on the whole network in various wave environments or construct more complex systems with versatile functions by designing the component. Moreover, the self-assembly strategy proposed here is possible to be applied to other large-scale constructions in the sea as it offers a facile fabrication method in water environment.

3. Conclusions

In summary, a self-assembly, self-hearable and reconfigurable TENG network based on an encapsulated high-performance TENG unit for water wave energy harvesting is presented. The macroscopic self-assembly network of TENG units is enabled by a rationally designed SAM-joint which operates on a self-adaptive mechanism of the pole and an anisotropic restriction on the degree of freedom, and the pattern of the self-assembly network can be tuned by the amount of SAM-joints on each unit. The network also demonstrates the capabilities of self-healing up ruptures and facile reconfiguration. Such high autonomous features greatly enhance the mechanical robustness of the network as a large-scale marine construction, facilitating the fabrication and maintenance. The 3D electrode structure of the TENG unit can boost the charge and power output by greatly increasing the contact interface. A maximum peak power of 8.75 mW and maximum average power of 2.33 mW for each TENG unit are attained with ideal agitations in air, corresponding to a peak power density of 32.6 W m^{-3} and an average power density of 8.69 W m^{-3}, respectively. A demonstrative network including 18 TENG units is shown to efficiently harvest water wave energy with a high average power of 9.89 mW, which are used for self-powered sensing and wireless signal transmission. The self-assembly TENG network as a robust and high-performance structure should pave a new avenue towards large-scale utilization of the wave power, providing an inexhaustible renewable and clean energy source for the human society.

4. Experimental section

4.1. Fabrication of the TENG ball

As shown in Fig. S10 in the Supplementary Information, thirteen transverse electrode plates and four longitudinal electrode plates were prepared by the printed circuit board (PCB) fabrication technics with copper patterns on double sides. Such electrode plates were then spliced and welded together, forming a 3D electrode ball (66 mm in diameter) with a number of internal channels and a pair of 3D copper electrodes on the substrates. 65 g FEP pellets with a diameter of 4 mm were intercalated into the internal channels, filling about half of the volume of each channel. The 3D electrode ball was then encapsulated tightly by a spherical polypropylene (PP) shell and sealed with water-proof glue to form the TENG ball (80 mm in diameter).

4.2. Fabrication of the SAM-joint

For the four-joint unit, a 15 mm wide Poly(ethylene terephthalate) (PET) belt with four equally-spaced circular holes (7 mm in diameter) was prepared at first (not shown in Fig. 1b for simplicity). A spherical NdFeB magnet (Shenzhen Friendship Magnetism Technology) with a diameter of 8 mm was placed into the groove of an acrylic holder as shown in Fig. 1b. To avoid corrosion in water, the magnet was covered with crystal wax (3M) Four such holders containing spherical magnets were then glued to the PET belt in alignment with the holes, thus the magnets were encapsulated between the PET belt and the holders and could rotate freely. Four acrylic limit blocks with a thickness of 3 mm were glued to the other side of the PET belt near the holes, opposite to the holders. For units with other amounts of joints, the fabrication were conducted similarly.

4.3. Fabrication of the self-assembly TENG unit

The above fabricated PET belt was adhered around the periphery of the TENG ball with the SAM-joints equally distributed, forming the self-assembly TENG unit. For tests in water, small blocks of expandable polyethylene (EPE) foams and a mass block (37 g) were adhered to the TENG ball to ensure a designed orientation of the TENG ball in water. In most of the self-assembly experiments without measuring electrical outputs, a model ball which has the same diameter as the sealed TENG ball was adopted to fabricate the self-assembly unit for simplicity.

4.4. COMSOL simulation

The magnetic force of spherical magnets with different diameters were numerically calculated by a commercial software COMSOL. The remanent flux density and the relative magnetic permeability for the magnet were set as 1.17 T and 1.05 respectively. The magnetic force was calculated at different distances.

4.5. Characterization

For the experiments in air, the TENG was agitated by a linear motor (LinMot E1100) as shown in Figs. S11 and a pinion and rack mechanism was adopted to convert linear movement to rotation to realize the pitching motion. The experiments in water was conducted in a wave tank with wave makers. The output current and transferred charges of the TENG were measured by an electrometer (Keithley 6514). The magnetic force was measured by a load cell (FUTEK LRM200). A high-speed camera (Photron FASTCAM Mini AX) was adopted to record the self-adjusting behavior of the spherical magnets in the joints while approaching each other.

Author contributions

L. X. and Z. L. W. conceived the idea. L. X. and P. L. designed the TENG ball. X. Y. fabricated the device. X. Y., L. X., W. Z., Y. B., J. L. and J. C. did the experiment. L. X., X. Y. and Z. L. W. discussed the data and prepared the manuscript. Z. L. W. guided the whole project.

Acknowledgments

The research was supported by the National Key R & D Project from Minister of Science and Technology, China (2016YFA0202704), National Natural Science Foundation of China (Grant No. 51605033, 51735001, 51432005, 5151101243, and 51561145021), China Postdoctoral Science Foundation (Grant No. 2015M581041), and Beijing Municipal Science and Technology Commission (Grant No. Z171100000317001, Z171100002017017, and Y3993113DF).

Appendix A. Supplementary data

Supplementary data to this article can be found online at https://doi.org/10.1016/j.nanoen.2019.03.054.

References

[1] E. Callaway, Nature 450 (2007) 156–159.
[2] J. Scruggs, P. Jacob, Science 323 (2009) 1176–1178.
[3] J. Tollefson, Nature 508 (2014) 302–304.
[4] A. Khaligh, O.C. Onar, Energy Harvesting: Solar, Wind, and Ocean Energy Conversion Systems, CRC Press, Boca Raton, 2009.
[5] Z.L. Wang, T. Jiang, L. Xu, Nano Energy 39 (2017) 9–23.
[6] S.H. Salter, Nature 249 (1974) 720–724.
[7] A.F.D. Falcao, Renew. Sust. Energy Rev. 14 (2010) 899–918.
[8] F.R. Fan, Z.Q. Tian, Z.L. Wang, Nano Energy 1 (2012) 328–334.
[9] Z.L. Wang, Faraday Discuss 176 (2014) 447–458.
[10] Z.L. Wang, Nature 542 (2017) 159–160.
[11] Z.L. Wang, Mater. Today 20 (2017) 74–82.
[12] Y.L. Zi, H.Y. Guo, Z. Wen, M.H. Yeh, C.G. Hu, Z.L. Wang, ACS Nano 10 (2016) 4797–4805.
[13] L. Xu, T. Jiang, P. Lin, J.J. Shao, C. He, W. Zhong, X.Y. Chen, Z.L. Wang, ACS Nano 12 (2018) 1849–1858.
[14] J. Chen, Y. Huang, N.N. Zhang, H.Y. Zou, R.Y. Liu, C.Y. Tao, X. Fan, Z.L. Wang, Nat. Energy 1 (2016) 16138.
[15] J.Q. Xiong, P. Cui, X.L. Chen, J.X. Wang, K. Parida, M.F. Lin, P.S. Lee, Nat. Commun. 9 (2018) 4280.
[16] Y. Lee, S.H. Cha, Y.W. Kim, D. Choi, J.Y. Sun, Nat. Commun. 9 (2018) 1804.
[17] X.F. Wang, S.M. Niu, Y.J. Yin, F. Yi, Z. You, Z.L. Wang, Adv. Energy Mater. 5 (2015) 1501467.
[18] J.F. Shin, W. Xu, M. Zanella, K. Dawson, S.N. Savvin, J.B. Claridge, M.J. Rosseinsky, Nat. Energy 2 (2017) 16214.
[19] K.M. Gattas-Asfura, C.A. Constantine, M.J. Lynn, D.A. Thimann, X.J. Ji, R.M. Leblanc, J. Am. Chem. Soc. 127 (2005) 14640.
[20] K.F. Wagenbauer, C. Sigl, H. Dietz, Nature 552 (2017) 78–83.
[21] G.M. Whitesides, B. Grzybowski, Science 295 (2002) 2418–2421.
[22] M. Rubenstein, A. Cornejo, R. Nagpal, Science 345 (2014) 795–799.
[23] A. Harada, R. Kobayashi, Y. Takashima, A. Hashidzume, H. Yamaguchi, Nat. Chem. 3 (2011) 34–37.
[24] Y. Wang, X.Y. Wei, S.Y. Kuang, H.Y. Li, Y.H. Chen, F. Liang, L. Su, Z.L. Wang, G. Zhu, ACS Nano 12 (2018) 441–447.
[25] S. Miyashita, R. Pfeifer, Adapt. Behav. 20 (2012) 117–130.
[26] C. Zhang, W. Tang, C.B. Han, F.R. Fan, Z.L. Wang, Adv. Mater. 26 (2014) 3580–3591.
[27] Y.L. Zi, S.M. Niu, J. Wang, Z. Wen, W. Tang, Z.L. Wang, Nat. Commun. 6 (2015) 8376.
[28] T. Zhou, L.M. Zhang, F. Xue, W. Tang, C. Zhang, Z.L. Wang, Nano Res 9 (2016) 1442–1451.
[29] S.M. Niu, S.H. Wang, L. Lin, Y. Liu, Y.S. Zhou, Y.F. Hu, Z.L. Wang, Energy Environ. Sci. 6 (2013) 3576–3583.
[30] Y.L. Zi, S.M. Niu, J. Wang, Z. Wen, W. Tang, Z.L. Wang, Nat. Commun. 6 (2015) 8376.
[31] F.B. Xi, Y.K. Pang, W. Li, T. Jiang, L.M. Zhang, T. Guo, G.X. Liu, C. Zhang, Z.L. Wang, Nano Energy 37 (2017) 168–176.

Xiaodan Yang received her Bachelor of Science in Xidian University in 2016. She is currently pursuing a master's degree in Beijing Institute of Nanoenergy and Nanosystems under the supervision of Prof. Zhong Lin Wang. Her research interests include blue energy and self-powered electronics.

Dr. Liang Xu received his Ph.D. degree from Tsinghua University (THU) in 2012, with awards of Excellent Doctoral Dissertation of THU and Excellent Graduate of Beijing. From 2015, he worked as a postdoctoral fellow under the supervision of Prof. Zhong Lin Wang in Beijing Institute of Nanoenergy and Nanosystems (BINN), Chinese Academy of Sciences. He is now an associate professor in BINN. His research interests include triboelectric nanogenerators and self-powered systems, blue energy, fundamental tribological phenomena, scanning probe microscopy and molecular dynamics simulation.

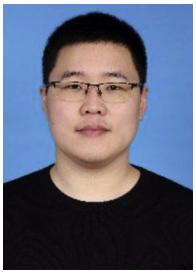

Dr. Pei Lin received his Ph.D. degree in Materials Science and Engineering (MSE) from University of Science and Technology Beijing in 2016. He then joined the group of Prof. Zhong Lin Wang at Beijing Institute of Nanoenergy and Nanosystems, CAS as a postdoctoral fellow. His research interests focus on the fields of piezotronics/piezophototronics for application in smart human-machine interfacing and self-powered systems.

Wei Zhong received his undergraduate degree in Chemical Engineering and Technology from Jishou University, China in 2015. Now he is a doctoral candidate in Beijing Institute of Nanoenergy and Nanosystems, Chinese Academy of Sciences. His research interests are mainly focused on triboelectric nanogenerators and special materials.

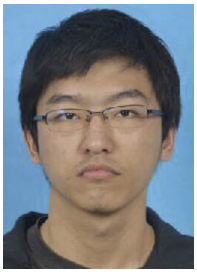

Yu Bai received his undergraduate degree from North China University of Technology in 2015, and his major is Mechanical Engineering. Now he is a Ph.D. candidate in Beijing Institute of Nanoenergy and Nanosystems, Chinese Academy of Sciences. His research interests are focused on air purification, blue energy harvesting, and self-powered systems.

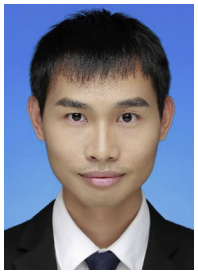

Dr. Jianjun Luo received his B.S. degree in Applied Chemistry from Jinan University in 2013, and his Ph.D. degree in Condensed Matter Physics from University of Chinese Academy of Sciences in 2018. He is now a post-doctoral fellow in Beijing Institute of Nanoenergy and Nanosystems, Chinese Academy of Sciences, under the supervision of Prof. Zhong Lin Wang. His research interests include triboelectric nanogenerators, self-powered systems and supercapacitors.

Jian Chen is presently a Ph.D. candidate at Beijing Institute of Nanoenergy and Nanosystems, CAS, under the supervision of Professor Zhong Lin Wang. His research focuses on energy harvesting and self-powered system.

Prof. Zhong Lin Wang received his Ph.D. from Arizona State University in physics. He now is the Hightower Chair in Materials Science and Engineering, Regents' Professor, Engineering Distinguished Professor and Director, Center for Nanostructure Characterization, at Georgia Tech. Prof. Wang has made original and innovative contributions to the synthesis, discovery, characterization and understanding of fundamental physical properties of oxide nanobelts and nanowires, as well as applications of nanowires in energy sciences, electronics, optoelectronics and biological science. His discovery and breakthroughs in developing nanogenerators established the principle and technological roadmap for harvesting mechanical energy from the environment and biological systems for powering a personal electronics. His research on self-powered nanosystems has inspired the worldwide effort in academia and industry for studying energy for micro-nano-systems, which is now a distinct disciplinary in energy research and future sensor networks. He coined and pioneered the field of piezotronics and piezophototronics by introducing piezoelectric potential gated charge transport process in fabricating new electronic and optoelectronic devices. Details can be found at: www.nanoscience.gatech.edu.